An Efficient Optimization Framework Including Mobile Generators for Resilience-Oriented Long-Term Planning

E. Ciapessoni, D. Cirio, A. Pitto
Power System Development Dept.
Ricerca sul Sistema Energetico - RSE S.p.A.
Milano, Italy
emanuele.ciapessoni@rse-web.it

***Abstract*—Achieving resilience against severe weather is a prominent objective for power system operators. This paper presents an extension of a Cost-Benefit Analysis (CBA) framework based on Optimization via Simulation (OvS) for selecting the optimal portfolio of resilience enhancement measures. The optimal mix is determined using an efficient two-step procedure based on the generalized pattern search technique. The framework quantifies risk indicators considering climate change models and simulating cascading outages. The methodology extends the analysis to address a new threat, i.e. the strong wind threat, and models the Mobile Emergency Generators (MEGs), which represent a hybrid measure as MEG procurement implies investment costs like passive measures, but this measure is activated, like other active measures, to improve system's response to severe outages. Simulations on a medium-sized IEEE test system demonstrate the approach's effectiveness in identifying the best measure portfolio, including MEGs, based on costs and climate projections, for both wet snow and wind threats.**

***Index Terms*—resilience, cost-benefit analysis, long-term grid planning.**

I. INTRODUCTION

The increasing emphasis on power system resilience, defined by CIGRE as "the ability to limit the extent, severity and duration of system degradation following an extreme event" [1], is driving Transmission and Distribution System Operators (TSOs/DSOs) to develop dedicated resilience plans [2], where Cost–Benefit Analysis (CBA) represents a key tool for prioritizing interventions [3]. Resilience measures are commonly classified as passive (system hardening) or active (enhanced system operation). Despite extensive research on cost-effective resilience enhancement [4]–[12], including risk-based assessment [5] and optimization-based hardening strategies [6], [7], [10], several limitations remain. In particular, most approaches assess a predefined and limited set of measures, thus preventing the identification of an optimal combination of passive and active actions. Furthermore, the impact of Climate Change (CC) on hazard characteristics over long-term planning horizons is often neglected or oversimplified [4], [6], [7], [11], [12]. In addition, contingency analysis is typically performed using simplified Optimal Power Flow (OPF) models, which do not capture the actual behavior of protection and control systems, leading to inaccurate representations of cascading failures [6], [7], [11], [12].

These gaps were addressed in [13] through a framework that: (i) applies Optimization via Simulation (OvS) to identify cost-effective portfolios of hardening and operational measures; (ii) incorporates probabilistic modeling of CC effects; (iii) exploits a cascading failure simulator for realistic system response assessment; and (iv) employs a generalized pattern search algorithm suitable for large-scale grids. The framework was demonstrated for the wet-snow threat, considering selected passive measures (antitorsional devices and support reinforcements) and conventional active measures (e.g., generator redispatch and load shedding).

In parallel, Mobile Emergency Generators (MEGs) have gained attention as an effective option for mitigating severe outages by supplying emergency power and reducing unserved energy. Existing studies address MEG pre-positioning and routing in distribution networks [14], transmission-level placement based on fragility scenarios [15], multi-stage stochastic planning with nonanticipativity constraints [16], and MEG sizing for service restoration [17]. However, these contributions generally do not include long-term cost–benefit assessments nor detailed cascading failure modeling.

This paper extends the methodology proposed in [13] by: (i) incorporating the strong wind threat; (ii) expanding the set of countermeasures to explicitly account for MEG procurement and positioning costs within a CBA framework; and (iii) improving the robustness of the solution algorithm. By embedding MEGs in a climate-aware OvS process, their costs and benefits can be consistently evaluated alongside alternative resilience measures, rather than being treated as a standalone operational problem.

The paper is organized as follows: Section II recalls the original CBA methodology, Section III presents its evolution. Section IV discusses the application results on a case study. Section V concludes.

979-8-3315-8138-1

II. Recalls on the Original CBA Methodology

This section recalls the methodology proposed in [13], for the selection of active and passive measures to enhance power system resilience in long-term planning. Two indicators based on actualized benefits ($B_{TOT,act}$) and actualized costs ($C_{TOT,act}$), are considered, i.e. the Total Net Benefit (TNB)

$$TNB = B_{TOT,act} - C_{TOT,act} \quad (1)$$

and the System Utility Index (SUI), also called Benefit-to-Cost Ratio (BCR) in ENTSO-E CBA [3]:

$$SUI = B_{TOT,act} / C_{TOT,act} \quad (2)$$

The methodology workflow adopts a scenario-based approach to manage the long-term variability and uncertainty of operational conditions, threat scenarios, and climate change. Threat intensities are modeled by a Generalized Extreme Value distribution for each climatological period of e.g. 5-10 years. The CBA is performed considering a reduced set of representative long-term scenarios $n = 1, \ldots, N$. For each climatological period, a scenario is defined by a triple $\{L, G; Th\}$ of stochastic discrete variables: (a) Load level L, $i_L = 1\ldots, N_L$, (b) Renewable generation level G, $i_G = 1\ldots, N_G$, (c) threat stress level Th (e.g., wet-snow intensity), $i_{Th} = 1\ldots, N_{Th}$.

Each scenario n has absolute probability π_n derived from a Gaussian-copula model capturing correlations among variables L, G, Th. For each scenario, a screened set C_n of critical N-k contingencies is identified. Vulnerability curves evaluated at threat level th yield component failure probabilities. The latter are then combined to obtain the probability of each contingency j in scenario n. For each contingency $j \in C_n$ with probability π_j, the ENS (Energy Not Served) is computed using a cascading-failure quasi-static simulator [18].

The optimization problem is formulated using binary decision variables to describe the space of possible active and passive measures $\{\Omega, \Phi_C, \Phi_P\}$. The objective function (OF) is to maximise the SUI or TNB indexes over $\{\Omega, \Phi_C, \Phi_P\}$ as in (3):

$$\max_{\{\Omega,\Phi_C,\Phi_P\}} SUI \quad \text{or} \quad \max_{\{\Omega,\Phi_C,\Phi_P\}} TNB \quad (3)$$

where Ω is the set of passive hardening measures on components selected based on subsection III.A.1; Φ_P represents the preventive measures aimed at improving system security under given operating conditions; and Φ_C is the set of possible corrective measures aimed to limit impact of contingencies after they occur in the scenario (possibly modified by preventive measures).

The constraints concern: (a) maximum costs for each typology of measure with respect to the relevant budgets; (b) the persistence of a hardening measure over subsequent climatological periods; (c) the rate of improvement of the failure return period of an asset in case of application of the hardening measure; (d) the maximum admissible residual EENS (Expected Energy Not Served); (e) technical limits related to active measures. The resulting binary non-linear optimization problem is solved using the Generalized Pattern Search algorithm [19], as detailed in [13].

III. Extension of the Methodology

A. Modeling of a new threat and countermeasures

The first extension concerns the extension of the CBA methodology to the "strong wind" threat, with focus on indirect effects of wind (i.e. actions on interfering vegetation). In fact, wind speeds which cause a significant probability of indirect effects typically lie in a range of 60-80 km/h [20], where the direct actions have a negligible probability to cause line damages, due to design criteria [21].

1) Integration of the New Vulnerability Models

The vulnerability model for overhead lines (OHLs) to indirect effects is described in [20], which provides one vulnerability curve for each span of a line. Combining these curves with the probability distribution of the threat (e.g., wind speed) yields span failure Return Periods (RP), which can be aggregated into line failure RP. The RP is the average time between two consecutive occurrences of a threat exceeding a severity threshold or a component failure. The average value $\hat{V}$ of the normal distribution Φ (with standard deviation $\sigma_{\hat{V}}$) of the vulnerability for the whole line is set based on (4), where P_s is the probability of exceeding the critical value $L_{critical}$ (for example 100 km/h in the case of indirect effects of wind threat) on at least one of the groups of spans of the line considered in the RP calculation.

$$\hat{V} \quad s.t. \quad \Phi^{-1}\left(\min\left(1, \frac{1}{RP \cdot P_s}\right), \hat{V}, \sigma_{\hat{V}}\right) = L_{critical} \quad (4)$$

The candidate lines for reinforcement are selected based on a ranking list with increasing failure RP values.

2) Extension of the Set of Passive Countermeasures

The list of measures for wind threat is partially different from the one deployed for wet snow threat. In particular: (1) tree pruning or trimming of the potentially interfering vegetation is a maintenance-based measure, thus only an OPEX cost is defined in terms of amu/km, with amu standing for arbitrary monetary unit, (2) the conversion from overhead lines to cables is introduced as a further passive measure.

B. MEG Modeling: Assumptions, Criteria for Candidate Nodes and Integration in the CBA

For the integration in the optimal mix methodology, a MEG is characterized by the level of installed power (in MW) and the grid node where it is normally located in each climatological period. A MEG location far from the nodes which experience more frequent energy disruptions results in higher costs of transport and lower CBA indices. The set of decision variables for the optimization-based CBA framework is thus extended to include MEG installed power and location. To this purpose, a set of candidate nodes is selected in the pre-optimization phase: specifically, all the load nodes which experienced a load disruption in at least one of the multiple contingencies selected by the algorithm in the analysis of the base case are considered as candidate nodes. Possibly, other more complex criteria can be applied such as the site accessibility, the criticality of the served loads, etc.

1) Logistic and availability model: assumptions

The logistic model of the MEGs assumes an artificially increased unitary cost for transport to quantify potential threat-induced problems in accessing to the faulty components in the CBA. A more complete probabilistic model which quantifies the dependence of the whole asset recovery process timing on

979-8-3315-8138-1

weather conditions has been proposed in [22] for operational planning purposes. Such model, if applied to long-term planning applications, would call for the Monte Carlo sampling of many realizations of the space-time evolution of the threat during the same event, to cope with the uncertainties at long-term planning level. To preserve efficiency the proposed approach limits the threat uncertainty modeling to the quantification of the probability of overcoming the critical value of the stress variable as indicated in subsection III.A.1.

2) Representing the Relevant Decision Variables

MEG's power rating is discretized, enabling a binary representation: a maximum number $N_{MEG,c}$ of MEGs with individual rating P_{meg} is supposed to be installed at each node $c \in C$, being C the set of candidate nodes selected based on the highest probabilities of load disruption events over analysed contingencies. Any number of MEGs n_c between 0 and $N_{MEG,c}$ is given in (5).

$$n_c = \left(b^{(c)}_{M_{TOT}-1} b^{(c)}_{M_{TOT}-2} \dots b^{(c)}_0\right)_2 = \sum_{h=0}^{M_{TOT}-1} b^{(c)}_h \cdot 2^h \tag{5}$$

where $M_{TOT} = \max_{c \in C} M_c$ being M_c the number of binary variables needed to represent the integers up to $N_{MEG,c}$ and $b_h^{(c)}$ represents the value 0/1 for the h-th coefficient of the base-2 representation for n_c. Given the basic rating P_{meg}, the total amount of MWs of MEGs at node c is given by $n_c \cdot P_{MEG}$. Considering the N_p climate periods, vector x_{MEG} in (6) is defined to represent the number of MEG units for each candidate node $c = 1 \dots N_c$ and each climatological period p.

$$x^{(p)}_{MEG} = \left[b^{(1,p)}_{M_{TOT}-1} \dots b^{(1,p)}_0, \dots, b^{(c,p)}_{M_{TOT}-1} \dots b^{(c,p)}_0, \dots, b^{(N_c,p)}_{M_{TOT}-1} \dots b^{(N_c,p)}_0 \right]$$
$$x_{MEG} = \left[x^{(1)}_{MEG} \dots x^{(N_p)}_{MEG} \right] \tag{6}$$

Vector x_{MEG} is integrated into an augmented array of decision variables in the optimization problem in subsection II.

Given the gas turbine's 11-year service life [23] and the adopted 10-year climatological period, no persistence constraints are applied to MEGs. New capital costs are needed for procurement in consecutive periods.

3) Assessing Impact of MEG Installation and Operation

A MEG located at a certain grid node can be used at that node or at other nodes, provided that enough time is available to transfer the component. All this requires an upgrade of the quasi-static cascading outage simulator in section II, based on the following indications:

1. After the application of the initiating contingency, the simulator performs a check about the presence of isolated nodes or islands provoked by the outages (it is assumed that no lines are available to reconnect the island to the main grid). If yes, the tool computes the costs to feed the load at the isolated bus with a MEG located at a specific candidate node (either the isolated node itself or other nodes) and with the given installed power from subsection III.B.2). In particular, the tool considers: (a) the cost for the MEG transport from the candidate node to the isolated node, expressed in amu/km. This cost is null if the MEG is already at the isolated node (or in the specific island); (b) the start-up and fuel cost for MEG, in amu/MWh.
2. In case of transport of MEG from far nodes to the affected node, the transport time must be accounted for, which limits the benefit of using MEG (during the transport time, the isolated substation experiences total load disruption).
3. After that, the tool considers the cascading outages potentially provoked by the initiating contingency. In this case, the system response, driven by potential cascading outages or power imbalances, evolves in a few minutes, a time interval shorter than the time needed to transport the MEG from far nodes to the affected island: the algorithm only accounts for the activation of MEGs already present in the islands which need to support the power balance.
4. Finally, the chosen impact indicator i.e. Energy Not Served (ENS), is calculated considering a conventional duration of the interruption, set to 16 hours in line with indications from the TSO [22]. The dispatch rule for MEG consists in matching as much load as possible to assure the balance in the affected islands. A maximum autonomy time is assumed based on the power/energy sizing of the devices, assuming the lack of continuity in fuel supply.

The MEG costs are counted in terms of both procurement and operational costs, specifically as "corrective measure" costs as they are used after the occurrence of contingencies.

C. Enhancing the Robustness of the Solution Algorithm

One limitation highlighted in [13] for the SUI-based optimization consists in the fact that a very cost-effective set of measures (i.e. which leads to the highest SUI) often implies a very limited reduction in residual EENS. For this reason, a constraint on the maximum admissible residual EENS, $EENS_{MAX}$, has been introduced for the SUI-based optimization: however, setting the $EENS_{MAX}$ threshold independently from the EENS in the base case, $EENS_0$, may bring to infeasibility of the solution. To solve this issue, the constraint on maximum admissible residual EENS is relaxed and replaced by introducing a multiplying factor DF, as presented in (7), to modify the current SUI-based OF in (3).

$$DF = \frac{EENS_0 - EENS}{\max(EENS_0, EENS_{max}) - \min(EENS_0, EENS_{max})} \tag{7}$$

Equation (7) holds valid for both cases: in fact, DF is positive when $EENS$ is lower than $EENS_0$, and the closest the distance between $EENS_0$ and $EENS_{MAX}$ the largest the sensitivity of DF factor from the distance $EENS_0 - EENS$.

The modified OF_{new} for SUI-based optimization becomes:

$$OF_{new} = OF_{original} \times DF = \frac{Benefits}{Costs} \times DF \tag{8}$$

where $OF_{original}$ is the ratio between Benefits and Costs.

IV. Case Study

The proposed approach has demonstrated its ability to deliver computationally efficient, sub-optimal yet operationally valuable solutions for large-scale power systems, as shown in [13] considering the wet-snow threat.

A. Test System and Base Cases

For the sake of clarity, presented extensions are tested on the IEEE 118 bus test system [24], which provides a good trade-off between tractability and size a medium-sized test system. In the test system generators at buses 46, 49, 54, 59, 61, 65, 91, 100, 103 and 105 represent equivalent renewable power injections. The georeferenced one-line diagram of the grid used for the present application is recalled in Figure 1a.

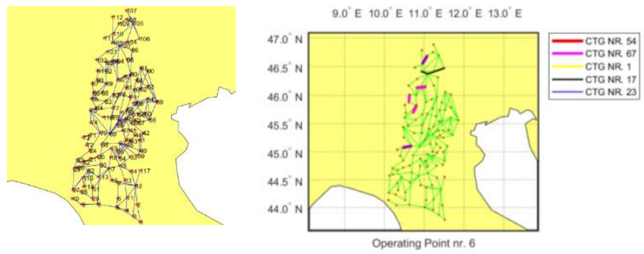

(a) (b)

Figure 1. (a) One-line georeferenced diagram of 118-bus IEEE test system; (b) visualization of failed components Visualization of top-ranking contingencies in the base case for scenario 6 in the 1st climatological period.

The application of the framework to the strong wind threat is considered. The Fast Forward Method [25] is used to identify 24 representative Threat/Renewable-Generation/Load scenarios (4 operating points × 3 climatological periods × 2 threat conditions). Scenarios with intense threat correspond to indices 5–8, 13–16, and 21–24 for the first, second, and third climatological periods, respectively. The adopted datasets include yearly load demand and renewable generation profiles from [26] and [27], and Complementary Cumulative Distribution Functions (CCDFs) of exceeding the critical wind speed threshold (100 km/h) for past and future periods (2021-30, 2031-40, 2041-50) from [28]. MEG parameters adopted in the simulations are reported in TABLE I, while cost assumptions for all other measures are taken from [13].

TABLE I. MEG PARAMETERS.

Quantity	Unit	Value
Capital cost for installation	amu/MW	10^3
Fuel cost	amu/MWh	10
O&M cost	% of capital cost/yr	2
Transport cost	amu/km	0.1
Service life	year	10

The critical wind speed used in simplified vulnerability models of the assets is 100 km/h. The base cases (in case of no countermeasures) have a residual EENS of 2036 MWh, with a maximum ENS among N-k contingencies of 1540 MWh. Figure 1b highlights the failed components associated to the 5 top-ranking contingencies in the base case for scenario 6 related to the 1st climatological period. Given similar locations for faulty components also for the 2nd and 3rd periods, the optimization identifies a set of candidate nodes for MEG pre-positioning, mainly located in the Northern part of the grid. Regarding the solution algorithm options, the maximum calculation time is set to 2 hours (7200 s) and the maximum number of OF evaluations is set to 3000. Parameter $EENS_{MAX}$ in (8) is set equal to 1000 MW.

B. *Optimizing the Countermeasures for Strong Wind Threat*

TABLE II and TABLE III report the set of active and passive measures identified, respectively in case of TNB-based and SUI-based optimization. TABLE IV reports the results on MEGs' installation for each climatological period, assuming that old MEGs are replaced by new ones from one climatological period to the following one.

TABLE II. SET OF MEASURES IDENTIFIED WITH THE TNB-BASED OPTIMIZATION IN CASE OF "STRONG WIND" THREAT. C_VM = COSTS FOR VEGETATION MAINTENANCE [AMU]; C_PRC_MEG = COSTS FOR MEG PROCUREMENT; C_CM = COSTS FOR CORRECTIVE MEASURES [AMU].

<table>
<tr><th></th><th colspan="4">Costs [amu]
(Upgraded Line | MEG Bus | Scenario ID)</th></tr>
<tr><th>Measures</th><th>1st period</th><th>2nd period</th><th>3rd period</th><th>Total</th></tr>
<tr><td>C_VM [amu]
(upgraded line)</td><td>-</td><td>$7.96\cdot10^5$
(75-118)</td><td>$2.06\cdot10^6$ (53 -54)
$7.96\cdot10^5$ (75-118)</td><td>$3.65\cdot10^6$</td></tr>
<tr><td>C_PRC_MEG
[amu] (bus)</td><td>$7.2\cdot10^4$ (112)
$7.2\cdot10^4$ (76)
$4.8\cdot10^4$ (95)</td><td>$7.2\cdot10^4$ 112)
$7.2\cdot10^4$ (76)
$4.8\cdot10^4$ (95)</td><td>$9.6\cdot10^4$ (112)
-
$1.2\cdot10^4$ (95)</td><td>$4.92\cdot10^5$</td></tr>
<tr><td>C_CM [amu]
(scenario)</td><td>$1.29\cdot10^3$ (5)
$1.39\cdot10^4$ (6)
$2.36\cdot10^3$ (7)
$1.00\cdot10^3$ (8)</td><td>$9.83\cdot10^2$ (13)
$3.89\cdot10^3$ (14)
$5.79\cdot10^3$ (15)
$1.42\cdot10^3$ (16)</td><td>$1.68\cdot10^2$ (21)
$1.30\cdot10^3$(22)
$8.92\cdot10^2$ (23)
$3.36\cdot10^2$ (24)</td><td>$3.33\cdot10^4$</td></tr>
</table>

TABLE III. SET OF MEASURES IDENTIFIED WITH THE SUI-BASED OPTIMIZATION IN CASE OF "STRONG WIND" THREAT.

<table>
<tr><th></th><th colspan="4">Costs [amu]
(MEG bus | Scenario ID)</th></tr>
<tr><th>Measures</th><th>1st period</th><th>2nd period</th><th>3rd period</th><th>Total</th></tr>
<tr><td>C_PRC_MEG
[amu] (bus)</td><td>$3.6\cdot10^4$ (52)</td><td>$3.6\cdot10^4$ (52)</td><td>$2.4\cdot10^4$ (52)</td><td>$9.6\cdot10^4$</td></tr>
<tr><td>C_CM [amu]
(scenario)</td><td>$4.20\cdot10^2$ (5)
$2.84\cdot10^3$ (6)
$1.39\cdot10^3$ (7)
$3.48\cdot10^2$ (8)</td><td>$3.42\cdot10^2$ (13)
$2.31\cdot10^3$ (14)
$1.73\cdot10^3$ (15)
$3.43\cdot10^2$ (16)</td><td>$6.48\cdot10^1$ (21)
$6.65\cdot10^2$ (22)
$4.70\cdot10^2$ (23)
$7.87\cdot10^1$ (24)</td><td>$1.10\cdot10^4$</td></tr>
</table>

TABLE IV. AMOUNT OF EMERGENCY POWER FROM, AND LOCALIZATION OF MEGS FOR THE THREE CLIMATOLOGICAL PERIODS. (A) TNB-BASED AND (B) SUI-BASED OPTIMIZATION FOR "STRONG WIND" THREAT.

(a)	1st period		2nd period		3rd period	
	Rating [MW]	Bus	Rating [MW]	Bus	Rating [MW]	Bus
MEG 1	60	112	60	112	80	112
MEG 2	60	76	60	76	10	95
MEG 3	40	95	40	95	-	-

(b)	1st period		2nd period		3rd period	
	Rating [MW]	Bus	Rating [MW]	Bus	Rating [MW]	Bus
MEG 1	30	52	30	52	20	52

The residual EENS is reduced by 96%, from 2036 MWh to 81 MWh, confirming the effectiveness of the selected measures. The optimal solution combines the installation and use of three MEGs in all climatological periods with vegetation trimming outside the ROW of line 53–54 in period 3 and line 75–118 in periods 2 and 3. The resulting total TNB over 30 years is $1.135\cdot10^8$ amu, while the total SUI is 119.8 (corresponding to an annual SUI of about 3.9), a value considered satisfactory by TSOs. As expected, line conversion to cables is not selected due to its high capital cost. The SUI-based optimization suggests installing a single MEG at bus 52 in all periods, with lower power ratings than the TNB-based solution (up to 30 MW versus 60 MW). This option is more cost-effective (30-year SUI increasing to over 818) at the expense of a higher residual EENS (1095 MWh), which still represents a 46% reduction relative to the base case.

TABLE V summarizes SUI, TNB, and residual EENS for two MEG installation cost assumptions (10^3 and 10^4 amu/MW) and for both objective functions.

979-8-3315-8138-1

TABLE V. SUI, TNB AND RESIDUAL EENS INDICATORS AFTER THE DEPLOYMENT OF THE SET OF MEASURES OBTAINED FROM TNB-BASED AND SUI-BASED OPTIMIZATION, FOR TWO INSTALLATION COSTS (10^3 AMU/MW AND 10^4 AMU/MW), APPLIED TO "STRONG WIND" THREAT.

	TNB OF		**SUI OF**	
Installation costs / **Indicator**	10^3 amu/MW	10^4 amu/MW	10^3 amu/MW	10^4 amu/MW
SUI [-]	119.8	47.1	818	91.4
TNB [amu]	$1.135 \cdot 10^8$	$9.908 \cdot 10^7$	$5.847 \cdot 10^7$	$5.713 \cdot 10^7$
Residual EENS [MWh]	80.98	114.35	1095.7	1147.4
Total Costs [amu]	$1.816 \cdot 10^6$	$4.066 \cdot 10^6$	$6.493 \cdot 10^4$	$5.406 \cdot 10^5$
Total Benefits [amu]	$1.153 \cdot 10^8$	$1.032 \cdot 10^8$	$5.853 \cdot 10^7$	$5.767 \cdot 10^7$

An increase of installation costs determines a higher impact on SUI indexes which undergoes a 60% and 88% reduction respectively for TNB- and SUI-based optimization, while TNB decreases by 13% (2%) for TNB- (SUI-) based optimization.

V. CONCLUSIONS

The paper has presented an extension of a CBA framework for resilience-oriented long-term planning, introducing wind threat, MEG modeling and an improved formulation of SUI-based OF. Simulations applied to a medium sized IEEE test system indicate that the modification of the objective function determine a satisfactory balance between cost-effectiveness and resilience improvement. Simulations also confirm the higher cost-effectiveness of the SUI-based optimization relative to the TNB-based approach, at the expense of a higher residual EENS. MEGs are consistently selected by both optimization targets, affirming their technical and economic viability as a countermeasure. The resulting methodology is a computationally efficient solution for long-term resilience planning. Future work will include an extensive simulation campaign on large power systems, the integration of a more complex asset recovery model, and the extension of the methodology to new threats such as floods.

ACKNOWLEDGMENT

This work has been financed by the Research Fund for the Italian Electrical System under the Three-Year Research Plan 2025-2027 (MASE, Decree n.388 of November 6th, 2024), in compliance with the Decree of April 12th, 2024.

REFERENCES

[1] CIGRE WG C4.47, "Defining power system resilience," *Electra.*, no. 316, pp. 1–3, 2019.

[2] M. Papic, S. Ekisheva, J. Robinson, and B. Cummings, "Multiple outage challenges to transmission grid resilience," in *Proc. 2019 IEEE PES General Meeting*, Atlanta, GA, USA, Aug. 2019, pp. 1–5.

[3] ENTSO-E, "4th ENTSO-E Guideline for cost-benefit analysis of grid development projects", 2024.

[4] M. Panteli, D. N. Trakas, P. Mancarella, and N. D. Hatziargyriou, "Power Systems Resilience Assessment: Hardening and Smart Operational Enhancement Strategies," *Proc. IEEE*, vol. 105, pp. 1202–1213, 2017. doi: 10.1109/jproc.2017.2691357.

[5] E. Ciapessoni, D. Cirio, M. Lacavalla, G. Pirovano, A. Pitto, E. Carlini, et al., "Application of a multi-hazard risk-based resilience assessment methodology to real cases in the Italian Transmission System," Proc. of 2024 CIGRE Session, Paris, 2024, pp.1-13.

[6] R. Moreno and G. Strbac, "Integrating high impact low probability events in smart distribution network security standards through CVAR optimisation," in *Proc. IET Int. Conf. Resilience of Transmission and Distribution Networks (RTDN)*, Birmingham, UK, Sep. 2015, pp. 1–6.

[7] T. Lagos, R. Moreno, A. N. Espinosa, M. Panteli, R. Sacaan, F. Ordonez, H. Rudnick, and P. Mancarella, "Identifying Optimal Portfolios of Resilient Network Investments Against Natural Hazards, With Applications to Earthquakes," *IEEE Trans. Power Syst.*, vol. 35, pp. 1411–1421, 2019. doi: 10.1109/tpwrs.2019.2945316.

[8] E. A. M. Cesena et al., "Quantifying the Impacts of Modelling Assumptions on Accuracy and Computational Efficiency for Integrated Water-Energy System Simulations Under Uncertain Climate," *IEEE Trans. Sustain. Energy*, vol. 13, pp. 1370–1382, 2022.

[9] K. Anderson, X. Li, S. Dalvi, S. Ericson, C. Barrows, C. Murphy, and E. Hotchkiss, "Integrating the Value of Electricity Resilience in Energy Planning and Operations Decisions," *IEEE Syst. J.*, vol. 15, pp. 204–214, 2020. doi: 10.1109/jsyst.2019.2961298.

[10] B. Zou, C. Wang, Y. Zhou, J. Wang, C. Chen, and F. Wen, "Resilient co-expansion planning between gas and electric distribution networks against natural disasters," *IET Gener. Transm. Distrib.*, vol. 14, pp. 3561–3570, 2020. doi: 10.1049/iet-gtd.2019.0569.

[11] H. Ranjbar, S. H. Hosseini, and H. Zareipour, "Resiliency-oriented planning of transmission systems and distributed energy resources," *IEEE Trans. Power Syst.*, vol. 36, pp. 4114–4125, 2021.

[12] L. Souto, J. Yip, W. Y. Wu, B. Austgen, E. Kutanoglu, J. Hasenbein, and S. Santoso, "Power system resilience to floods: Modeling, impact assessment, and mid-term mitigation strategies," *Int. J. Electr. Power Energy Syst.*, vol. 135, p. 107545, 2022.

[13] E. Ciapessoni, D. Cirio, A. Pitto, "A Cost–Benefit Analysis Framework for Power System Resilience Enhancement Based on Optimization via Simulation Considering Climate Changes and Cascading Outages", *Energies*, Vol. 16, no. 5160, pp. 1-39, 2023.

[14] S. Lei, J. Wang, C. Chen and Y. Hou, "Mobile Emergency Generator Pre-Positioning and Real-Time Allocation for Resilient Response to Natural Disasters," in *IEEE Transactions on Smart Grid*, vol. 9, no. 3, pp. 2030-2041, May 2018, doi: 10.1109/TSG.2016.2605692.

[15] I. Satkauskas, J. Maack, M. Reynolds, D. Sigler, K. Panda, and W. Jones, "Emergency Generation Asset Positioning for Resilient Transmission Grid Operation: Preprint," National Renewable Energy Laboratory (NREL), Golden, CO,USA,NREL/CP-2C00-84712, 2023.3

[16] G. Zhang, F. Zhang, X. Zhang, Z. Wang, K. Meng, Z. Y. Dong, "Mobile Emergency Generator Planning in Resilient Distribution Systems: A Three-Stage Stochastic Model with Nonanticipativity Constraints," *IEEE Trans. Smart Grid*, vol. 11, no. 6, pp. 4847–4859, Nov. 2020.

[17] N. Bhusal, M. Gautam and M. Benidris, "Sizing of Movable Energy Resources for Service Restoration and Reliability Enhancement," *2020 IEEE Power & Energy Society General Meeting (PESGM)*, Montreal, QC, Canada, 2020, pp. 1-5

[18] E. Ciapessoni, D. Cirio, and A. Pitto, "Cascadings in large power systems: Benchmarking static vs. time domain simulation," in *Proc. 2014 IEEE PES GM Conf.*, Washington, DC, USA, Jul. 2014, pp. 1–5.

[19] V. Torczon, "On the Convergence of Pattern Search Algorithms," *SIAM J. Optim.,* vol. 7, no. 1, pp. 1–25, 1997.

[20] E. Ciapessoni, D. Cirio, A. Pitto, G. Pirovano and M. Sforna, "Modelling the vulnerability of overhead lines against tree contacts for resilience assessment," *2020 Int. Conf. on Probabilistic Methods Applied to Power Systems (PMAPS)*, Liege, Belgium, 2020, pp. 1-6.

[21] CEI (Italian Electrotechnical Committee) Std 11-4, "Norme tecniche per la costruzione di linee elettriche aeree esterne", (in Italian), 1998-9.

[22] E. Ciapessoni, D. Cirio, A. Pitto, and M. Sforna, "A quantitative methodology to assess the process of service and infrastructure recovery in power systems," *Electric Power Syst. Res.*, vol. 189, p. 106735, 2020, doi: 10.1016/j.epsr.2020.106735.

[23] G. Badeer, "GE Aeroderivative Gas Turbines - Design and Operating Features," GE Power Systems, Evendale, USA, 2000.

[24] R. Christie, "Power Systems Test Case Archive," Aug. 1993. [Online]. Available: http://www.ee.washington.edu/research/pstca/

[25] H. Heitsch, W. Romisch, "Scenario Reduction Algorithms in Stochastic Programming," *Comput. Optim. and Appl.*, vol. 24, 2003, pp. 1-21.

[26] IEEE Probabilistic Methods Subcommittee, "IEEE Reliability Test System," in *IEEE Transactions on Power Apparatus and Systems*, vol. PAS-98, no. 6, pp. 2047-2054, Nov. 1979.

[27] Renewables.ninja. [Online]. Available: https://www.renewables.ninja/

[28] E. Ciapessoni, D. Cirio, A. Pitto, E. M. Carlini, et al. "An innovative methodology for risk-based resilience assessment to prioritize grid interventions against natural threats in the Italian power system," *Environment Systems and Decisions*, vol. 46, no. 1, pp. 4, Jan. 2026.